Environ Geol (2007) 52:831–842
DOI 10.1007/s00254-006-0525-5

ORIGINAL ARTICLE

Environmental monitoring of magnetic iron phases of urban water reservoir lake sediments (Taiaçupeba Lake, metropolitan region of São Paulo, Brazil) by using Mössbauer spectroscopy

D. R. Franco · T. S. Berquó · R. A. L. Imbernon · C. S. M. Partiti · J. Enzweiler

Received: 30 May 2006 / Accepted: 18 September 2006 / Published online: 11 October 2006

Abstract In the present work, we investigate the iron oxides and oxyhydroxides behavior and evolution, related to the geochemical behavior of some metals, which could be retained as solid phases in the sediments from an urban water reservoir lake, placed in Taiaçupeba, Great São Paulo, Brazil. These tasks were performed by the establishment of a procedure setting for environmental monitoring analysis through Mössbauer spectroscopy measurements associated to hysteresis loops measurements and chemical analysis [X-ray fluorescence (XRF)]. We inferred the possibility of goethite occurrence in broad particle size distribution (5–50 nm), and related to ferrihydrite, and small grain-size hematite (about 8 nm). The magnetometry results pointed to the paramagnetic/superparamagnetic behavior of the magnetic phases present in the samples and also suggested the occurrence of small grain-size magnetite. We also verified the presence of clay minerals related to Fe, as well as the occurrence of Fe^{3+} and/or Fe^{2+} in short-range structural order. Through a straight correlation among Mössbauer spectra data gained at $T = 77$ K and Al-metal, metal-Fe molar ratios, provided through XRF data, we found remarkable indications of interference on meta-stable phases evolution to its final products. Such results can be pointing for evidences about the possible isomorphic replacing and/or adsorption of Al and other metals in goethite and hematite.

Keywords Sediments · Water pollution · Iron-bearing phases characterization · Mössbauer spectroscopy · Metropolitan region of São Paulo

D. R. Franco (✉) · T. S. Berquó · C. S. M. Partiti
Laboratory of Magnetic Materials, Institute of Physics,
University of São Paulo—USP, C.P. 66318,
05389-970 São Paulo, SP, Brazil
e-mail: drfranco@iag.usp.br

R. A. L. Imbernon
Laboratory of Hydrogeochemistry, Institute of Geosciences,
University of São Paulo—USP, Rua do Lago 562,
05422-970 São Paulo, SP, Brazil

J. Enzweiler
Institute of Geosciences,
State University of Campinas—UNICAMP, C.P. 6152,
13083-970 Campinas, SP, Brazil

Present Address:
D. R. Franco
Department Geophysics, Institute of Astronomy,
Geophysics and Atmospheric Sciences,
University of São Paulo, R. do Matão 1226,
05508-900 São Paulo, SP, Brazil

Present Address:
T. S. Berquó
Institute for Rock Magnetism,
Department of Geology and Geophysics,
University of Minnesota, Minneapolis, MN, USA

Introduction

The problems concerning pollution in hydromorphic systems are related to the character of dynamic in ecosystems. Heavy metals are toxic to animals, humans, and aquatic life and their toxicity, even in trace quantities have the tendency to be bioaccumulated in the food chain. In human beings when ingested and inhaled in excessive amounts, heavy metals can affect the liver, brain, and lungs, although each metal causes its own characteristic symptoms. For instance, a large range is often observed in concentrations of heavy (or

trace) metals in water column, which shows biotic and/or abiotic dependence. Human contribution is the main abiotic factor for heavy metals and pollutants dispersion in water systems, as the case of Pb availability, which is 17 times greater than by natural events (Petrovsky and Ellwood 1999). In contrast, the recommendation for drinking water published by World Health organization (WHO) present the maximum acceptable concentration of 0.01 mg/L for lead.

Trace metals are often related to the lower ion fraction, which is dissolved in water column and rapidly adsorbed by sediments. As reported by Förstner et al. (1990), sediments of hydromorphic systems—seas, rivers, urban water reservoir lakes, and others—are integrator sites. Sediments can store metals and organic substances, delivering these materials to the aquatic biota or the water column, consequently playing an important role on the fate and transport of metals in such environments (Davis and Upadhyaya 1996; Dong et al. 2001). Therefore, it provides information about pollution related to these materials (Dauvalter and Rognerud 2001). Although some studies (e.g., Borgmann et al. 2001) indicate that heavy metals concentrations cannot be evaluated because of the large variations in trace metal availability in sediments, other authors (e.g., Trivedi et al. 2001) suggest that sediments could provide indications, at least of qualitative nature, concerning the re-availability potential and mobility of these elements. Such indications could be found, indirectly by different characterization techniques, through alterations in specified physical–chemical properties of some compounds, due to the possibility of interactions related to heavy metals concentration in soils and sediments.

Hydromorphic systems present hydrogeochemical conditions for chemical and microbial reactions, which could be understood through observation of iron-bearing phase precipitation. Iron compounds have been extensively studied since such precipitates can modify the hydraulic integrity in hydromorphic systems, affecting trends in pH, alkalinity, mineral precipitation, and microbial activity (Liang et al. 2000). Several studies have been performed in an attempt to understand such mechanisms, as well to identify chemical aspects in such conditions (Blowes et al. 2000; Liang et al. 2000).

Furthermore, geochemical stability of the heavy metals, which are detected in the sediments, could be related to the iron-bearing phases replacing and evolution. Some authors (Oliveira et al. 1996; Imbernon et al. 1999) reported that metals incorporated to Fe-phases structure (e.g., Cu, Ni, Co, Zn, and Pb) could generate distortions in unit cells of these materials. There are also indications that occurrence of phosphate in sediments decreases ferrihydrite transformation rates in other crystalline iron oxides, and affects the physical–chemical characteristics of oxides, which are made up in these processes (Gálvez et al. 1999b). Ford et al. (1999) also reported that some metals, which are incorporated or co-precipitated with ferrihydrite, could prevent the transformation in its final crystalline products, as goethite and hematite.

These factors suggest that identification and evaluation of iron-bearing phases in sediments can be employed as an important application of environmental geochemistry studies and environmental monitoring. In sediments, iron oxides and oxyhydroxides occur among the main compounds of the superficial layers of sediments, and it has been related to the control of metal availability in aquatic systems (Drodt et al. 1997; Ford et al. 1999; Van der Zee et al. 2005). Nevertheless, some characteristics related to these phases (e.g., large range of grain sizes, low crystallinity and high degree of isomorphic replacement of iron by other cations, as Al and Ni), generate several problems in characterization by traditional techniques (e.g., X-ray diffraction). Such features reveal that development of characterization studies for the identification of the iron-bearing phases in sediments has been a challenge and a request for detailed geochemical investigations. This is important in understanding the sedimentological settings and, nowadays, there is an increasing request for employment of combined characterization techniques, in order to investigate variations in levels of pollution and the time-dependence of the contamination processes in water urban supply systems.

In this work, we will present and discuss Mössbauer spectroscopy (MS) results, and complementary data provided by X-ray fluorescence (XRF) and hysteresis loops related to ground water sediments samples from an urban water reservoir lake, placed in Taiaçupeba, Metropolitan Region of São Paulo, Brazil (MRSP). Such reservoir contributes to the Alto Tietê System, and its watershed is being under intense pressure due to urban expansion (Braga et al. 2006). The aim of this study is to investigate the iron oxides and oxyhydroxides behavior and evolution, related to the geochemical behavior of trace metals, which are present in the sediments.

Sampling location—Taiaçupeba urban supply lake

Taiaçupeba urban water reservoir lake (Fig. 1), with 19.36 km^2 and volume of 88×10^6 m^3, is placed

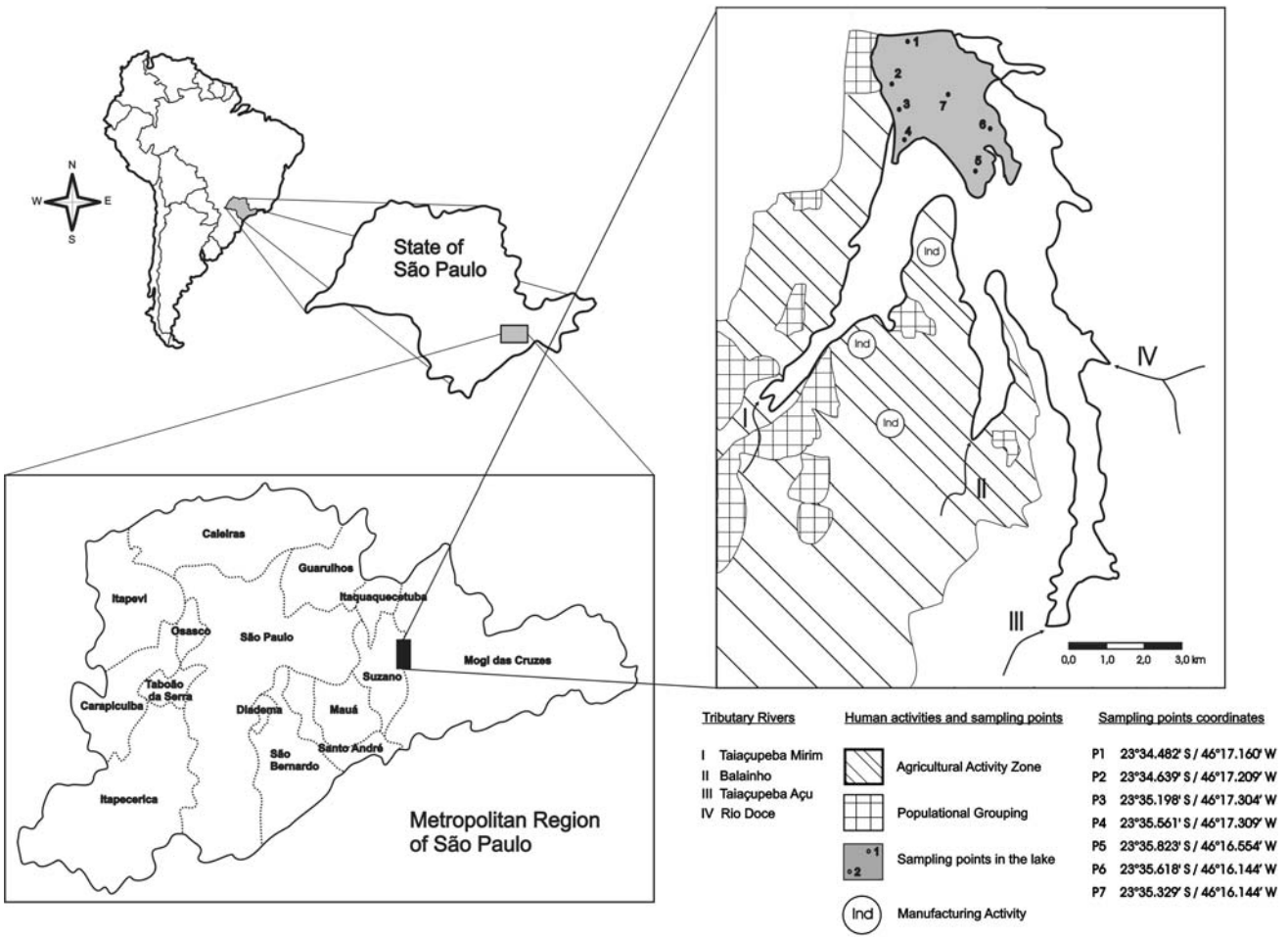

Fig. 1 Taiaçupeba urban water reservoir lake, showing sampling locations and tributary rivers disposition

between Suzano and Mogi das Cruzes cities, in the state of São Paulo, southeastern Brazil. As briefly discussed above, such reservoir is one of constituent of Alto Tietê System, which supplies 10 m^3/s to the MRSP, and can support further expansion up to 15 m^3/s (Braga et al. 2006). It contributes to the drinking water supply for about 2 million of inhabitants from eastern MRSP.

The use and employment of the surrounded area present a diversity of activities, which could generate environmental impacts on this aquatic system. Intensive agricultural activity areas surround the lake, especially between Taiaçupeba Mirim and Balainho tributary rivers. Such regions present a high-polluting potential (Franco 2002), due to an extensive use of organic/inorganic fertilizers. Some populational groupings belonging to Suzano and Mogi das Cruzes, and manufacturing activities (e.g., chemical, metallurgic, and paper industries) are mainly distributed close to Taiaçupeba Mirim River.

For the sampling, seven points were chosen obeying these location characteristics and water dynamics related to the tributary rivers of the lake. Point 1 (P1) and point 2 (P2) were sampled, respectively, at downstream and upstream of a water treatment station, for observing possible influences on water caption location. Point 3 (P3) had been chosen close to an agricultural activity area and populational grouping, for investigating possible influences of human activities on water quality. For the point 4 (P4), point 5 (P5), and point 6 (P6) the sampling were collected respectively close to the entrance of the Taiaçupeba-Mirim, Balainho and Taiaçupeba-Açú Rivers in the lake, for observing the contribution of carried materials by these rivers, which constitute Taiaçupeba lake. Point 7 (P7) had been chosen near to the center of the lake, due to the dynamics of deposition/formation of sediments.

During this study a very low-Fe content for sample P5 was verified. Such feature prevents a high-quality

iron phases characterization and correlation between XRF and Mössbauer data. Under such point of view, we will not discuss or present information of sample P5.

Experimental procedure

The seven sampling points in the lake were delimited with an employment of a GPS device (GPS data are exposed in Fig. 1). For a better homogenization, samples were collected with water (80 and 20%, respectively, related to the solid and liquid phase) from the water lake bottom (depth between 2 and 8 m), through the use of a depth sampler. Such samples were dried in air at constant temperature during 4–6 days, before melting and drizzling (bolter of 200 Mach) processes.

Mössbauer spectroscopy has been increasingly employed as an important tool in studies related to soils and sediments. MS could provide some information related to iron-bearing phases, such as particle size and grain-size distribution, oxidation degree, and distortions in the unit cells by iso/heteromorphic iron replacement, and the structural order of such phases, even if it occurs in low concentrations (Murad and Schwertmann 1980; Cornell and Schwertmann 1996). Furthermore, this spectroscopic technique, when combined to other traditional characterization techniques, can provide reliable qualitative results concerning the identification of the iron-bearing mineralogy. In recent studies, Bishop et al. (2001) and Guodong et al. (2001) have successfully used MS to characterize magnetic phases from lake sediments of Antarctica and southwestern China, respectively.

Mössbauer spectroscopy measurements were conducted with a Wissel equipment operating at constant acceleration, and used in transmission geometry with ^{57}Co/Rh source (initial intensity of 50 mCi). Mössbauer spectra (M-spectra) are presented at room temperature (RT), $T = 77$ and $T = 4.2$ K. Isomer shifts were calibrated relating to the velocity scale, using α-iron at RT. Fittings of M-spectra were performed following two distinct routines. The first one allowed fittings by Lorentzian lines in according to a crystallographic sites modeling, and corresponding to initial studies for testing the necessity of hyperfine fields and/or quadrupolar splitting fittings. We considered the importance of hyperfine field and/or quadrupolar splitting distributions (QSDs) as through the broadening lines subspectra analysis, as by the compatibility between two or more subspectra related to different iron-bearing phases, which show the same valence state and magnetic behavior at a given temperature. In these cases, the modeling of histogramical hyperfine field and QSDs were provided by the pair of least squares fitting software proposed by Brand (1987), and it has followed the preliminary results gained by the Lorentzian lines fitting. For the subspectra related to the same iron-bearing phases valence state, which shown narrowed line widths and mainly low contribution to the spectral relative areas at the three established temperatures, Lorentzians doublets and/or sextets were considered as pattern for concerning fittings.

For XRF analysis, samples were prepared as pressed pellets (40 mm diameter) by mixing 9.0 g sample and 1.5 g of wax powder (Hoechst, Frankfurt, Germany) during 5 min in a mixer (Spex, Metuchen, NJ, USA), and pressing at 119 MPa (60 s) with a semi-automatic press (HTP40, Herzog, Munic, Germany). A sequential XRF spectrometer PW 2404 was used (Philips, Eindhoven, The Netherlands), equipped with a 4 kW Rh tube and SuperQ 3.0 software. Matrix effects were corrected with UniQuant 5.0 (ODS, Beekbergen, The Netherlands) software, according to the method described by Enzweiler and Vendemiatto (2004).

Hysteresis loops measurements were performed to provide additional information about the iron-bearing phases, through the magnetic behavior interpretation at RT. It had been carried out using a superconducting quantum interference device (SQUID) magnetometer (Quantum Design, MPMS-XL, San Diego, CA, USA).

Table 1 Chemical analysis by X-fluorescence

Element (wt.%)	P1	P2	P3	P4	P6	P7
Si	11.0	18.6	19.1	16.2	18.0	20.2
Ti	0.68	0.58	0.53	0.38	0.50	0.60
Al	9.0	12.9	13.6	12.2	10.5	12.5
Fe	26.2	8.9	5.5	3.3	7.7	8.4
Mn	0.37	0.15	0.07	0.08	0.10	0.12
Ca	0.28	0.28	0.10	0.26	0.34	0.29
K	0.31	0.67	0.92	0.66	0.60	0.61
P	0.16	0.14	0.13	0.14	0.13	0.15
S	0.29	0.61	1.10	1.61	0.30	0.47
Zn	0.29	1.18	2.72	4.32	0.28	0.61
mg/kg						
Ba	171	227	302	180	255	240
Cr	69	81	73	64	75	86
Cu	105	400	1,420	1,810	76	137
Ni	74	60	102	101	22	41
Pb	31	65	99	128	41	52
V	159	162	146	99	134	165
Zr	153	215	200	79	138	223
TOC	9.81	9.24	6.48	15.10	10.63	10.32

TOC total organic carbon

Table 2 Al/(Al + Fe) and Zn/(Zn + Fe) molar ratios derived from chemical analysis

Sampling point	Al/(Al + Fe) (mol/mol)	Zn/(Zn + Fe) (mol/mol)
P1	0.416	0.009
P2	0.750	0.102
P3	0.837	0.297
P4	0.884	0.528
P6	0.738	0.030
P7	0.755	0.058

Results

Geochemical and mineralogical inferences through X-ray fluorescence data

Based on XRF results (Table 1) and correlations between each group of elements, it was possible to infer some aspects concerning the mineralogy, which occurs in the sediments. From Table 1 it can be verified that P1 is related to the main Fe content, which cannot be justified only as natural origin because of the verified high-level content. It could be explained due to a major mud contribution, related to the water treatment station, whereas iron sulfate is employed as flotation agent. Iron content showed an almost linear decreasing from P2 until P4 and then a trend of increase for the samples P6 and P7. This was observed for Al, Si, and K contribution—which could be related to iron oxides and/or oxyhydroxides as well silicate and aluminosilicate minerals, as reported above—a similar trend along the sampling. The presence of the metals Zn, Cu, Cr, Ni, V, and Pb was determined in all samples with the highest concentrations in the sampling points P2, P3, and P4. A positive correlation between S and Ba was found and it could indicate barite occurrence in the sampling points. Similar pattern is also verified for P and Ca, which is reasonable due to the agricultural activities surrounding the lake.

Furthermore, we calculated Al–Fe and Zn–Fe molar rates (Table 2), for checking a possible isomorphic replacing effects on iron oxides and/or oxyhydroxides in the related samples, as will be discussed later. It could be noted that the ratios Al–Fe and Zn–Fe had higher values on points P4 and P3, respectively. Its lower values were found on point P1, probably due to the higher Fe concentration on that sampling point.

Hysteresis loops

Hysteresis loops at RT were taken for all samples. The representative behavior found for samples P1, P4, and P7, are presented at Fig. 2. It is possible to notice that such hysteresis loops represent the overlap of at least three components corresponding to ferrimagnetic, paramagnetic and superparamagnetic phases. Such behavior can be also suggested by Mössbauer study (see below). In the case of sample P1, the major saturation magnetization value can be observed, perhaps because of a presumable high-ferrimagnetic phases concentration, as well higher iron content, as verified through XRF measurement of this sampling point. On the other hand, sample P4 has the lower saturation magnetization value, due to its higher presence of paramagnetic phases and lower iron

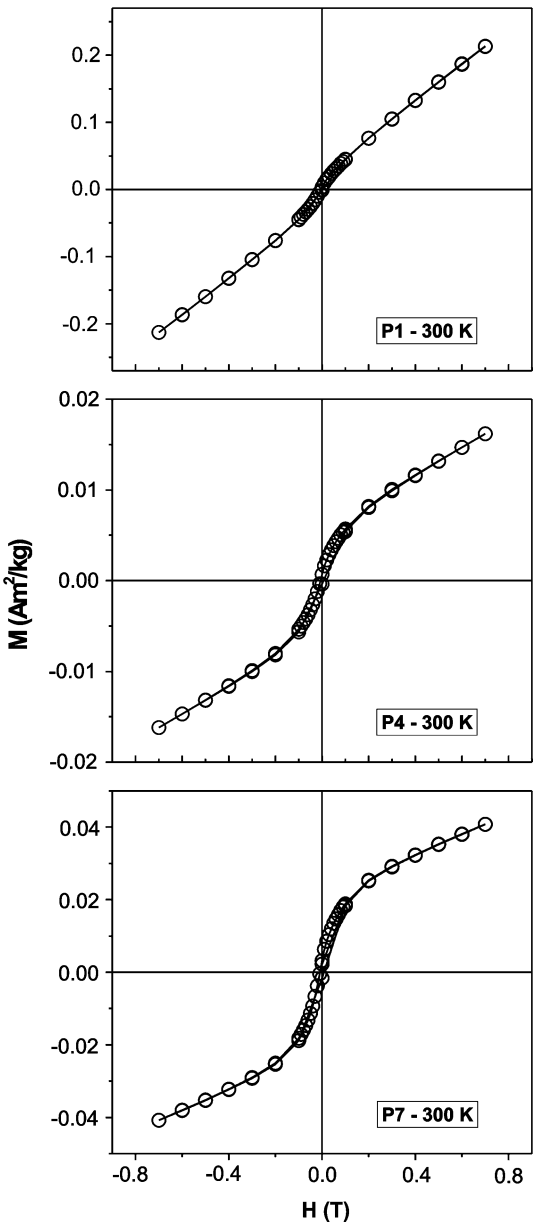

Fig. 2 Hysteresis loops (samples P1, P4, and P7) taken at RT

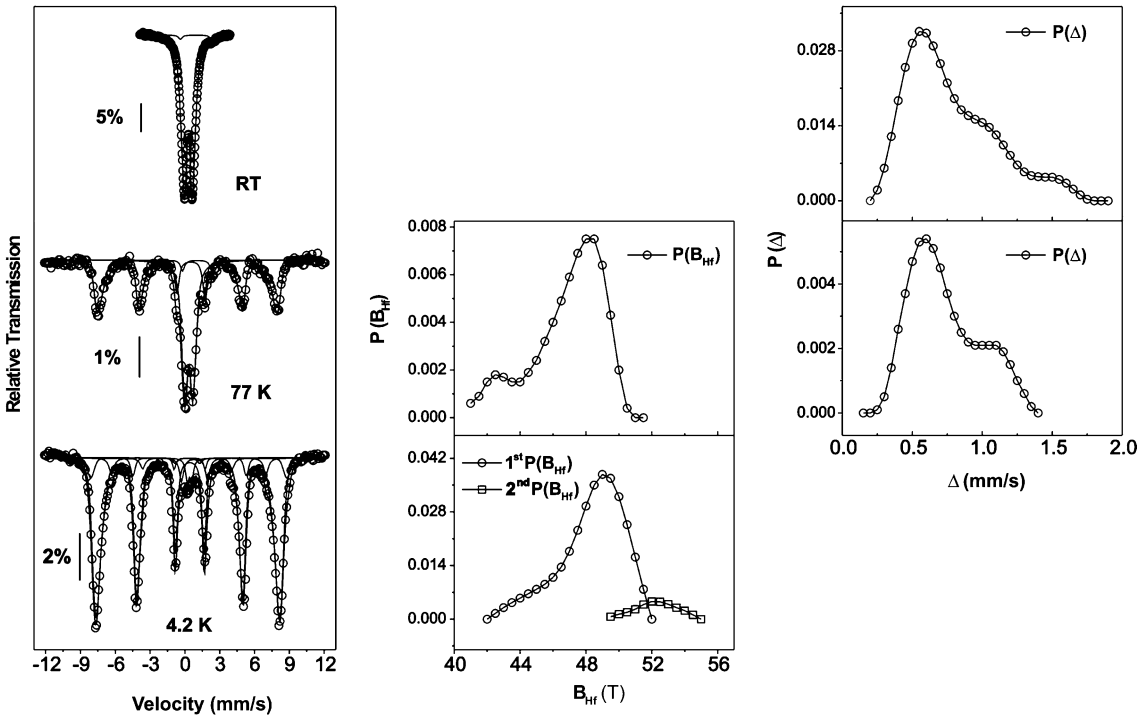

Fig. 3 Mössbauer spectra (sample P1) taken at RT, T = 77 and T = 4.2 K (*left column*). *Open circles* experimental points, *lines* the best fitting. *Center column* and *right column* are, respectively, magnetic hyperfine field distribution (B_{hf}) and quadrupolar distribution (Δ)

content. Remanent magnetization and coercive force values for all hysteresis loops of these samples are close to zero and in agreement with the main paramagnetic contribution (due to iron silicates) and with superparamagnetic iron phases (e.g., ferrihydrite) above blocking temperature. The sigmoidal behavior of these hysteresis loops is evident and also could be associated with high-coercivity iron phases, like hematite and goethite.

Mössbauer spectroscopy

Mössbauer spectra are showed in Figs. 3, 4, 5 and its hyperfine parameters in Tables 3, 4, 5. The evolution of M-spectra with temperature showed a clear evidence of iron oxides/oxyhydroxides presence going through magnetic ordering temperature. This is an effect related to particle size of the iron magnetic phases found in these sediments and/or association of iron replacing effects. Another important observation is that Fe^{2+}-doublet was present in all measurements for the studied samples. As will be presented below, based on M-fitting details, we can propose some correlations between components at different temperatures.

The Fe^{3+} QSD at RT is represented by one peak with a number of shoulders. Although a straight correspondence of QSD fitted and the iron oxides content is not possible, the occurrence of goethite in a large grain-size distribution, and presumably associated to iron replacement can be associated with such QSD parameters (Cornell and Schwertmann 1996). By RT measurements we can also suggest the occurrence of hematite, since in a smaller grain size (diameter smaller than 8 nm), through a doublet with quadrupolar splitting in the range 0.50–1.10 mm/s (Vandenberghe et al. 1990). Ferrihydrite through the RT (and T = 77 K) measurements is the other candidate. In general, ferrihydrite shows a high degree of structural disorder and a well-known stoichiometrical variability (Childs and Baker-Sherman 1984) with quadrupolar splitting values of 0.70–0.90 mm/s, and isomer shift values concerning Fe^{3+} in octahedral coordination of oxygen atoms (Bowen et al. 1993). Nevertheless, this behavior is compatible to the other iron-bearing phases in low-crystallinity state, producing broaden doublets and similar quadrupolar splitting to goethite and ferrihydrite (Murad 1998), which prevents unequivocal characterization of these phases. Furthermore, ferrihydrite is often related to its final products—as goethite—in soils and sediments. This association occurs in situ, where Fe^{2+} ions are rapidly oxidized in the presence of crystallization inhibitors,

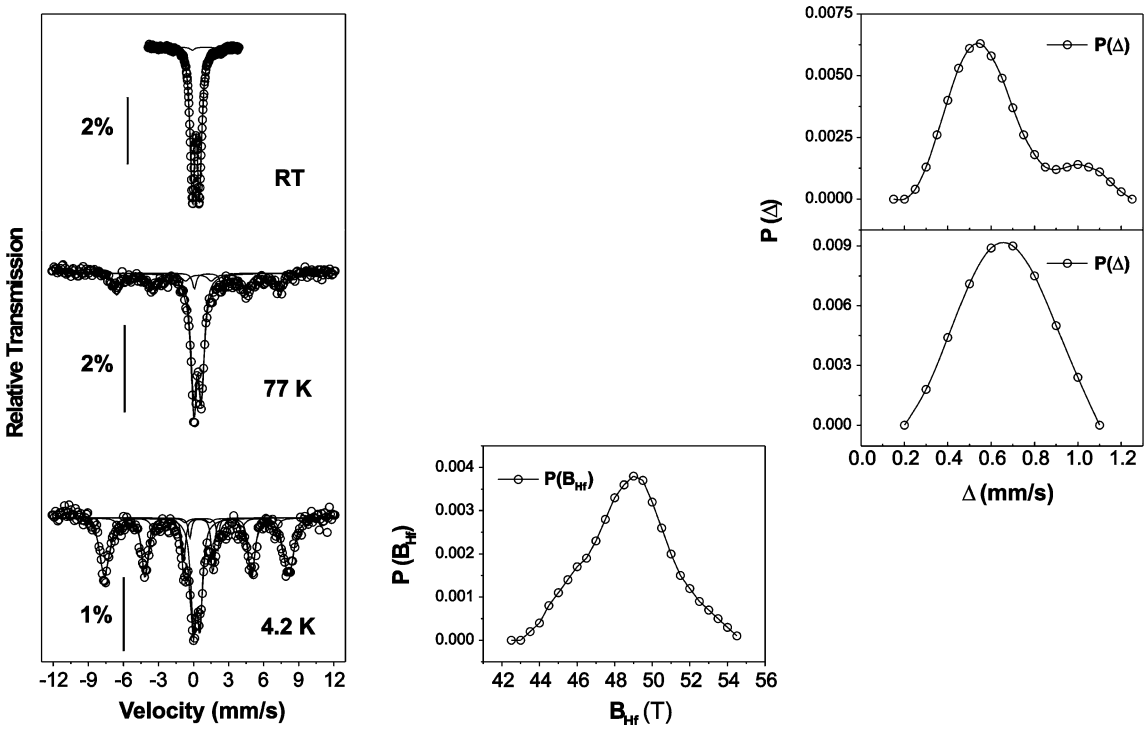

Fig. 4 Mössbauer spectra (sample P4) taken at RT, T = 77 and T = 4.2 K (*left column*). *Open circles* experimental points, *lines* the best fitting. *Center column* and *right column* are, respectively, magnetic hyperfine field distribution (B_{hf}) and quadrupolar distribution (Δ)

which promote ferrihydrite to goethite as precipitated primary phase (Cornell and Schwertmann 1996; Gálvez et al. 1999a).

The observed relative area decreasing of QSD at T = 77 K (in comparison with the corresponding subspectra at RT), and the presence of a sextet showing proportional magnetic ordering area is observed through the fitted hyperfine field distribution (HFD). The HFD, in general, also presented shoulders. For sample P7, the presence of a well-fitted peak (without shoulders) was noticed. The hyperfine parameters fitted support goethite contribution. Iron replacement by Al is quite probable, where the hyperfine field decreasing effects are often reported in literature (Cornell and Schwertmann 1996). Therefore, conditions about grain-size range and replacing effects related to this HFD would explain the observed superparamagnetism effects in a large grain-size range at RT measurements.

Through hyperfine parameters fitted for T = 77 K spectra, the inferred goethite-ferrihydrite association and nanometric grain-size hematite had found important evidences. Vandenberghe et al. (1990) reported that below 80 K doublets, which could be concerning low-crystallinity and/or high-replacing goethite could be pointing to ferrihydrite as well. Parameters fitted at this temperature had shown possible isomorphic replacement by Al for hematite. Such iron phase can retain more than 30 wt.% of Al, and this diamagnetic replacing produces reduction on Néel and Morin temperatures and hyperfine field (De Grave et al. 1988).

At T = 4.2 K measurements, iron-bearing phases, as well its associations, we found further evidences. At very low temperatures, hyperfine fields of goethite and ferrihydrite are similar—for ferrihydrite, it can be found values between 46 and 50 T, with small quadrupolar shift (between –0.02 and –0.1 mm/s), whereas goethite often shows saturation fields about 50.7 T, with narrowing resonance lines (Vandenberghe et al. 1990). Moreover, at T = 4.2 K, higher HFD average values are related to hematite but has been reported at this temperature hyperfine fields values around 50.4 T for synthetic nanoparticles of hematite (Murad and Johnston 1987; Cornell and Schwertmann 1996).

Clay minerals and/or phyllossilicates or else Fe^{3+} in a short-range structural arrangement are present through the parameters settings fitted at RT and T = 4.2 K, respectively. Clay minerals usually show

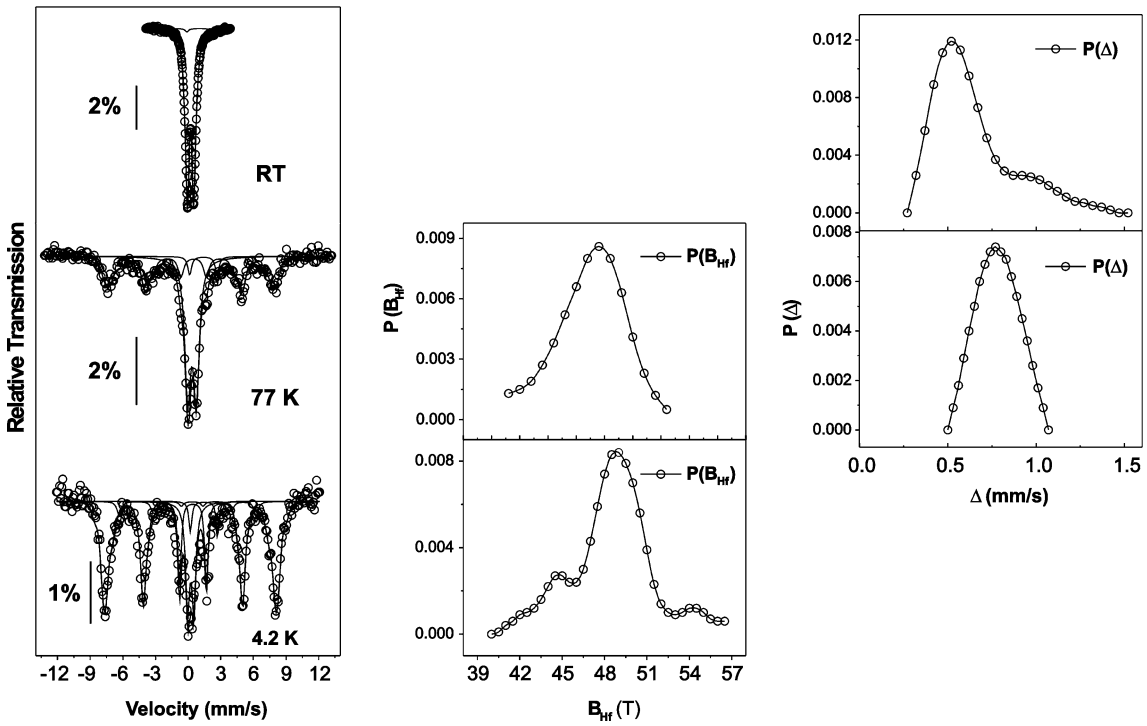

Fig. 5 Mössbauer spectra (sample P7) taken at RT, T = 77 and T = 4.2 K (*left column*). *Open circles* experimental points, *lines* the best fitting. *Center column* and *right column* are, respectively, magnetic hyperfine field distribution (B_{hf}) and quadrupolar distribution (Δ)

divalent and trivalent iron, which could occur in tetrahedral and/or octahedral sites and incorporated into hydroxide layers or else between layers as permutable cations. Nevertheless, such compounds often exhibit iron-poorly and rarely monophasic characteristics. Therefore, Fe^{3+}-QSD and Fe^{3+}-doublets at 4.2 K reinforce the presence of such materials, whereas iron-bearing phases reach full magnetic ordering at very low temperatures, without contributions for relative areas of such kind of subspectra. Kaolin extraction activities can be verified close to the water body, and the occurrence of kaolinite and illite in such sediments is expected. An additional contribution for non-ordering Fe^{3+}-subspectra is based on the effects of short-range structural ordering for different iron oxides occurrence. This occurs due to strong particle size decrease, which results in the individual characteristics disappearance (Mitra 1992), and consequently avoiding its magnetic ordering.

Finally, Fe^{2+}-doublets fitted for all measurements also could point to the presence of ''green-rusts,'' which are intermediary piroaurite-isostructural compounds among ferrous hydroxides and ferric oxyhydroxides (Benali et al. 2001). At T = 77 K, fitted quadrupolar doublet could point to these materials, probably related to piroaurite-compounds, which are often related to the presence of iron oxides and/or oxyhydroxides, as hematite and goethite (Mitra 1992).

QSD and HFD relative areas at T = 77 K versus Al–Zn and Zn–Fe molar ratios: an indicator for environmental monitoring on evolution of iron-bearing phases in sediments?

At T = 77 K M-measurements, ferrihydrite could be inferred by the QSD, because this phase does not show magnetic ordering, and goethite and/or hematite contribute for the magnetic ordering subspectra at the same temperature.

Prevention of ferrihydrite transformation in goethite/hematite can occur due to some metals, as Al and Zn, which could avoid a relative area increasing related to magnetic-ordered subspectra (sextets and/or HFD) rather than non-ordered subspectra (Fe^{3+}-doublets and/or QSD) at T = 77 K. It is important to note that Fe^{3+} and/or Fe^{2+}-bearing silicates can also present some levels of isomorphic replacing by metals (Dunn 1987; Blot and Imbernon 2000). However, these phases never have contributed to the magnetic-ordered subspectra.

Table 3 Mössbauer parameters taken from fittings of sampling points P1 and P2

Sample	Temperature	B_{hf} (T)	Δ (mm/s)	δ (mm/s)	Γ (mm/s)	RA (%)	Description
P1	RT	–	0.55 (5)	0.391 (4)	–	64	(a)
		–	0.95 (5)	0.391 (4)	–	26	(b)
		–	1.45 (5)	0.391 (4)	–	8	(c)
		–	2.68 (3)	1.04 (2)	–	2	(d) (e) (f) (k)
	77 K	42.5 (5)	–0.29 (1)	0.478 (4)	–	7	(g)
		48.0 (5)	–0.29 (1)	0.478 (4)	–	45	(h) (c)
		–	0.60 (5)	0.462 (4)	–	35	(i)
		–	1.05 (5)	0.462 (4)	–	10	(b)
		–	2.52 (9)	1.18 (5)	0.4 (F)	3	(d) (e) (f) (k)
	4.2 K	41.2 (1)	0.12 (3)	0.41 (1)	0.48 (F)	6	(b)
		49.0 (5)	–0.167 (3)	0.467 (3)	–	81	(a) (c)
		52.0 (5)	–0.07 (2)	0.502 (3)	–	7	(j)
		–	0.38 (2)	0.53 (1)	0.34 (F)	2	(k) (l)
		–	2.25 (2)	0.96 (1)	0.44 (F)	4	(d) (e) (f) (k)
P2	RT	–	0.50 (5)	0.318 (3)	–	73	(a)
		–	0.90 (5)	0.318 (3)	–	23	(b)
		–	1.38 (5)	0.318 (3)	–	4	(c)
	77 K	42.5 (5)	–0.317 (4)	0.485 (4)	–	10	(g)
		48.0 (5)	–0.317 (4)	0.485 (4)	–	41	(h) (c)
		–	0.71 (2)	0.435 (4)	–	49	(i) (b) (m)
	4.2 K	43.3 (2)	–0.08 (5)	0.51 (3)	0.60 (F)	13	(b)
		49.0 (5)	0.21 (1)	0.466 (3)	–	67	(c)
		54.5 (5)	–0.21 (1)	0.466 (3)	–	3	(j)
		–	0.30 (4)	0.37 (2)	0.36 (F)	7	(m)
		–	0.75 (8)	0.436 (3)	–	7	(k)
		–	1.39 (8)	0.436 (3)	–	3	(l)

B_{hf} hyperfine field, Δ quadrupolar splitting, δ isomer shift, Γ line width, *RA* relative area of the subspectra. Errors are quoted within parentheses

Description: (a) Goethite (15–20 nm) with presumable associated replacing effect, (b) association goethite-ferrihydrite, (c) Nanometric and/or replaced hematite (about 8 nm), (d) iron sulphates, (e) ''green rusts,'' (f) Fe^{2+} sites related to clay minerals, (g) small grain-size goethite, with presumable higher replacing level, (h) higher grain-size and low-crystallized goethite, in a low-crystallization degree (intermediary grain-size goethite), (i) very small grain-size goethite (about 5–10 nm), (j) Relaxation effects due to Fe nanometric phases, presumably adsorbed by interlayed minerals, (k) Fe^{3+} sites related to clay minerals, (l) Fe^{3+} in short range structural ordering, (m) clay minerals showing presumable absence of Fe^{2+} octahedral coordination sites, (n) continuum of Fe^{3+} octahedral sites presumably related to nanometric gothite and/or hematite, showing high-replacing levels, (F) fixed parameter

Following these hypotheses, M-data provided to QSD relative area could provide information about ferrihydrite concentration, and samples in which QSD and HFD relative areas are respectively higher and smaller, could be related to higher Al and Zn rates. Therefore, we established a straight correlation among M-spectra data gained at $T = 77$ K (QSD and HFD relative areas) and Al–Zn, Zn–Fe molar ratios, provided through XRF data. This set of procedures aimed to investigate the possible influence of some cations on evolution of iron-bearing phases to its final products, as goethite and hematite, through the sampling points of the water reservoir lake.

Figure 6 shows an important decreasing in HFD relative area related to an increase in QSD relative area, from sampling point P1 to P4, related to an increase in Al–Fe and Zn–Fe molar ratios. This observed behavior is compatible to the evidence discussed above, whereas an increase in Al–Fe and Zn–Fe could point to higher rates of ferrihydrite conversion in goethite/hematite, which could be observed through the increase in relative area of magnetic-ordering subspectra at $T = 77$ K.

Conclusions

One of the major challenges faced for water systems managements in the large metropolitan regions around the world is the well-known high-growth rates, which generate several problems for a sustainable and efficient water supply. As discussed above, the Alto Tietê System (MRSP, Brazil) presents a watershed in an intensive pressure because of the human activities increasing, especially related to the urban and agricultural use of land. The degradation of the water

Table 4 Mössbauer parameters taken from fittings of sampling points P3 and P4

Sample	Temperature	B_{hf} (T)	Δ (mm/s)	δ (mm/s)	Γ (mm/s)	RA (%)	Description
P3	RT	–	0.55 (5)	0.318 (3)	–	81	(b)
		–	1.10 (5)	0.318 (3)	–	15	(c)
		–	2.26 (11)	1.11 (7)	0.53 (F)	4	(d) (e) (f) (k)
	77 K	43.4 (8)	–0.20 (6)	0.491 (4)	–	7	(g)
		49.0 (8)	–0.20 (6)	0.491 (4)	–	33	(c) (h)
		–	0.77 (7)	0.442 (4)	–	58	(b) (i)
		–	2.68 (24)	1.22 (11)	0.25 (F)	2	(d) (e) (f) (k)
	4.2 K	43.0 (2)	0.04 (5)	0.39 (3)	0.61 (F)	15	(b)
		46.0 (5)	–0.20 (1)	0.454 (3)	–	4	(b)
		49.0 (5)	–0.20 (1)	0.454 (3)	–	49	(c)
		53.0 (5)	–0.20 (1)	0.454 (3)	–	4	(j)
		–	0.20 (5)	0.413 (3)	–	12	(k) (l)
		–	1.95 (6)	1.12 (2)	0.36 (F)	6	(d) (e) (f) (k)
P4	RT	–	0.55 (5)	0.298 (3)	–	83	(b)
		–	1.10 (5)	0.298 (3)	–	15	(c)
		–	2.31 (18)	1.14 (9)	0.45 (F)	2	(d) (e) (f) (k)
	77 K	43.2 (9)	–0.12 (F)	0.55 (2)	0.8 (F)	33	(n) (c) (h)
		–	0.7 (1)	0.477 (2)	–	61	(b) (l) (k) (e)
		–	2.38 (10)	1.39 (6)	0.38 (F)	6	(d) (e) (f) (k)
	4.2 K	40.9 (5)	0.04 (7)	0.48 (4)	0.62 (F)	10	(j)
		49.0 (5)	–0.15 (2)	0.467 (3)	–	56	(b)
		–	0.56 (1)	0.40 (1)	0.53 (F)	30	(e) (k) (l)
		–	2.40 (5)	1.01 (3)	0.31 (F)	4	(d) (e) (k) (f)

B_{hf} magnetic hyperfine field, Δ quadrupolar splitting, δ isomer shift, Γ line width, *RA* relative area of the subspectra. Errors are quoted within parentheses

Description: (a) Goethite (15–20 nm) with presumable associated replacing effect, (b) association goethite-ferrihydrite, (c) Nanometric and/or replaced hematite (about 8 nm), (d) iron sulphates, (e) ''green rusts,'' (f) Fe^{2+} sites related to clay minerals, (g) small grain-size goethite, with presumable higher replacing level, (h) higher grain-size and low-crystallized goethite, in a low-crystallization degree (intermediary grain-size goethite), (i) very small grain-size goethite (about 5–10 nm), (j) Relaxation effects due to Fe nanometric phases, presumably adsorbed by interlayed minerals, (k) Fe^{3+} sites related to clay minerals, (l) Fe^{3+} in short range structural ordering, (m) clay minerals showing presumable absence of Fe^{2+} octahedral coordination sites, (n) continuum of Fe^{3+} octahedral sites presumably related to nanometric gothite and/or hematite, showing high-replacing levels, (o) iron sulphides, (F) fixed parameter

quality may be monitored in order to identify the processes of contamination, which could meaningfully alter this system in a near future, preventing extensive damages for surrounding ecosystems and public health hazards.

The MS data associated to the hysteresis loops of the sediment samples indicate a magnetic behavior of the iron-bearing phases. M-spectra taken at three different temperatures provide a good description of magnetic behavior dependent on temperature, typical of iron oxides and/or oxyhydroxides.

The $T = 77$ K M-spectra data fits data associated to XRF analysis also indicate an influence of the presence of some metals on the iron-bearing phases. For instance, the transformation of metastable phases (e.g., ferrihydrite) to goethite/hematite can be hindered by presence of Al, Zn or Cu. For sample P5, it was not possible a good characterization of the iron phases, as well a reliable correlation between XRF and M-data, because of the low-Fe content which was verified for this sampling point.

Nevertheless, it is also important to consider that the data collected on such sediments, which were verified by this study, shall not fully correspond to the geochemical behavior of metals for this urban reservoir lake. Therefore, we strongly suggest for future works the sampling and analysis of water surface and groundwater at the same sampling points. Such kind of study could provide a better understanding on metal bioavailability and/or incorporation by solid phases, as iron oxyhydroxides present in the sediments for this water system.

This work, based on M-measurements associated to XRF and hysteresis loops data, had successfully identified iron-bearing phases probably associated with other metals present in sediments of a water reservoir and showed the potential of such tools in environmental geochemistry studies and environmental monitoring.

Table 5 Mössbauer parameters taken from fittings of sampling points P6 and P7

Sample	Temperature	B_{hf} (T)	Δ (mm/s)	δ (mm/s)	Γ (mm/s)	RA (%)	Description
P6	RT	–	0.50 (5)	0.345 (4)	–	5	(b)
		–	1.05 (5)	0.345 (4)	–	13	(c)
		–	2.40 (16)	1.12 (10)	0.67 (F)	2	(d) (e) (f) (k)
	77 K	39.7 (3)	–0.26 (5)	0.455 (2)	–	7	(g)
		43.0 (3)	–0.26 (5)	0.455 (2)	–	32	(h)
		–	0.66 (7)	0.440 (2)	–	58	(b) (k) (e)
		–	2.68 (6)	1.09 (6)	0.4 (F)	3	(d) (e) (f) (k)
	4.2 K	44.0 (5)	–0.20 (2)	0.485 (3)	–	12	(j) (j)
		49.0 (5)	–0.20 (2)	0.485 (3)	–	59	(b) (c)
		46.3 (2)	0.30 (7)	0.29 (3)	0.40 (F)	9	(b) (j)
		–	0.50 (3)	0.38 (2)	0.52 (F)	18	(k) (e)
		–	2.40 (5)	1.21 (3)	0.32 (F)	2	(d) (e) (f) (k)
P7	RT	–	0.52 (5)	0.317 (3)	–	79	(b)
		–	0.97 (5)	0.317 (3)	–	19	(c)
		–	2.34 (5)	1.15 (4)	0.38 (F)	2	(d) (e) (f) (k)
	77 K	47.6 (8)	–0.25 (5)	0.520 (2)	–	42	(h) (c)
		–	0.77 (3)	0.494 (2)	–	53	(b) (k) (e)
		–	2.53 (7)	1.55 (4)	0.4 (F)	5	(d) (e) (f) (k)
	4.2 K	39.0 (4)	–0.41 (10)	0.29 (6)	0.47 (F)	6	(j)
		45.0 (5)	–0.22 (1)	0.463 (3)	–	13	(j)
		49.0 (5)	–0.22 (1)	0.463 (3)	–	54	(b)
		54.5 (5)	–0.22 (1)	0.463 (3)	–	5	(c)
		–	0.56 (2)	0.37 (1)	0.46 (F)	18	(n) (k) (e)
		–	2.49 (5)	1.58 (2)	0.33 (F)	4	(d) (e) (f) (k)

B_{hf} magnetic hyperfine field, Δ quadrupolar splitting, δ isomer shift, Γ line width, *RA* relative area of the subspectra. Errors are quoted within parentheses

Description: (a) Goethite (15–20 nm) with presumable associated replacing effect, (b) association goethite-ferrihydrite, (c) Nanometric and/or replaced hematite (about 8 nm), (d) iron sulphates, (e) ''green rusts,'' (f) Fe^{2+} site related to clay minerals, (g) small grain-size goethite, with presumable higher replacing level, (h) higher grain-size and low-crystallized goethite, in a low-crystallization degree (intermediary grain-size goethite), (i) very small grain-size goethite (about 5–10 nm), (j) Relaxation effects due to Fe nanometric phases, presumably adsorbed by interlayed minerals, (k) Fe^{3+} sites related to clay minerals, (l) Fe^{3+} in short range structural ordering, (m) clay minerals showing presumable absence of Fe^{2+} octahedral coordination sites, (n) continuum of Fe^{3+} octahedral sites presumably related to nanometric gothite and/or hematite, showing high-replacing levels, (F) fixed parameter

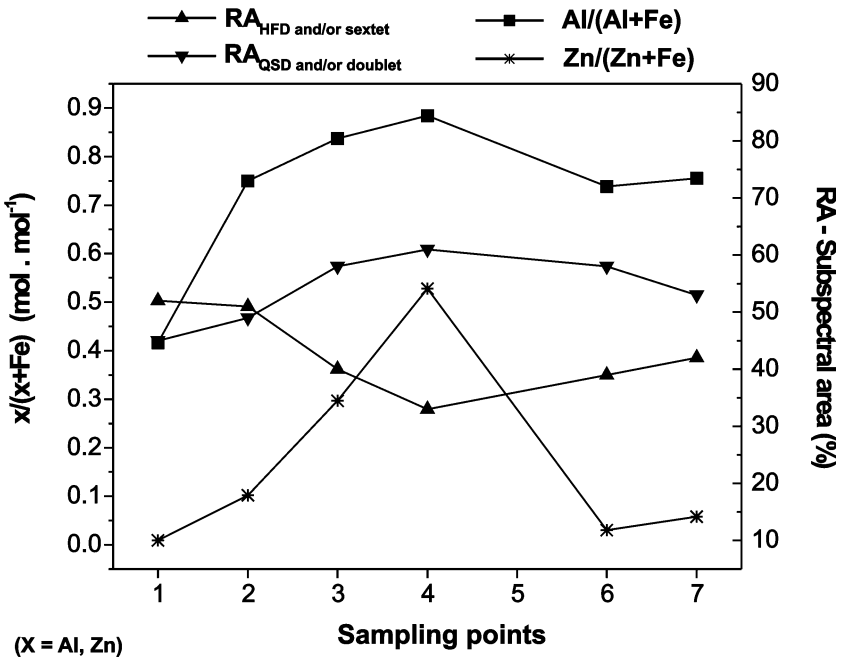

Fig. 6 Correlation between relative spectral areas of Fe^{3+} hyperfine field and quadrupolar distributions, and Al/(Al + Fe) and Zn/(Zn + Fe) molar ratios (respectively, related to $T = 77$ K Mössbauer fittings and XRF measurements), for all sampling points

Acknowledgments The authors are grateful to Prof. Dr. G. F. Goya, Prof. Dr. H. R. Rechenberg, Dr. J. A. H. Coaquira and Renato Cohen (Institute of Physics, University of São Paulo, Brazil) for the valuable contributions, which allowed the development of the present study. This work was partly supported by the Brazilian agencies CNPq and FAPESP (grants 00/06066-3 and 02/06480-0).

References

Benali O, Abdelmoula M, Refait P, Génin J-MR (2001) Effect of orthophosphate on the oxidation products of Fe(II)-Fe(III) hydroxycarbonate: the transformation of green rust to ferrihydrite. Geochem Cosmochim Acta 65(11):1715–1726

Bishop JL, Lougear A, Newton J, Doran PT, Froeschl H, Trautwein AX, Körner W, Koeberl C (2001) Mineralogical and geochemical analyses of Antartic lake sediments: a study of reflectance and Mössbauer spectroscopy and C, N, and S isotopes with applications for remote sensing on Mars. Geochem Cosmochim Acta 65(17):2875–2897

Blowes DW, Ptacek CJ, Benner SG, McRae CWT, Bennett TA, Puls RW (2000) Treatment of inorganic contaminants using permeable reactive barriers. J Contam Hydrol 45:123–137

Blot A, Imbernon RAL (2000) Caractérization par analyse thermique de la constitution cristallochimique de diverses chlorite zincifères. C R Acad Sci Paris Ser I 330:469–472

Borgmann U, Néron R, Norwood WP (2001) Quantification of bioavailable nickel in sediments and toxic thresholds to Hyalella azteca. Env Polit 111:189–198

Bowen LH, De Grave E, Vandenberghe RE (1993) Mössbauer effect studies of magnetic soils and sediments. In: Long GJ, Grandjean F (eds) Mössbauer spectroscopy applied to magnetism and materials science, vol 1. Plenun Press, New York, pp 115–159

Braga BPF, Porto MFA, Silva RT (2006) Water management in metropolitan São Paulo. Int J Water Res Dev 22(2):337–352

Brand RA (1987) Improving the validity of hiperfine field distributions from magnetic alloys—Part I: unpolarized source. Nucl Instrum Methods B 28:398–416

Cornell RM, Schewertmann U (1996) The iron oxides—structure, properties, reactions, occurrence and uses. Weinhein, New York, pp 573

Childs CW, Baker-Sherman JG (1984) N.Z. soil bureau scientific report 66, Department of Science and Industrial Research. Lower Hutt, New Zealand, pp 50

Dauvalter V, Rognerud S (2001) Heavy metal pollution in sediments of the Pasvik river drainage. Chemosphere 42(1):9–18

Davis AP, Upadhyaya M (1996) Desorption of cadmium from goethite (α-FeOOH). Water Res 30(8):1894–1904

De Grave E, Bowen LH, Vochten R, Vandenberghe RE (1988) The effect of crystallinity and Al substitution on the magnetic structure and Morin transition in hematite. J Magn Magn Mater 72:141–151

Dong D, Li Y, Zhang B, Hua X, Yue B (2001) Selective chemical extraction and separation of Mn, Fe oxides and organic material in natural surface coatings: application to the study of trace metal adsorption mechanism in aquatic environments. Microchem J 69:89–94

Drodt M, Trautwein AX, König I, Suess E, Bender Koch C (1997) Mössbauer spectroscopy studies on the iron forms of deep-sea sediments. Phys Chem Miner 24:281–293

Dunn PJ, Peacor DR, Ramik RA, Shu-Chun S, Rouse RC (1987) Franklinfurnaceite, a Ca-Fe^{3+}-Mn^{3+}-Mn^{2+} zincosilicate isotypic with chlorite, from Franklin, NJ. Am Miner 72:812–815

Enzweiler J, Vendemiatto MA (2004) Analysis of sediments and soils by X-ray fluorescence spectrometry using matrix corrections based on fundamental parameters. Geostand Geoanal Res 28:103–112

Förstner U, Schoer J, Knauth HD (1990) Metal pollution in the tidal Elbe river. Sci Total Environ 97/98:347–368

Ford RG, Kemner KM, Bertsch PM (1999) Influence of sorbate-sorbent interactions on the crystallization kinetcs of nickel—and lead—ferrihydrite coprecipitates. Geochim Cosmochim Acta 63:39–48

Franco DR (2002) Caracterização Magnética e Estrutural das Fases de Ferro em Sedimentos da Barragem de Taiaçupeba, São Paulo. MSc, University of São Paulo, Brazil (in Portuguese)

Gálvez N, Barrón V, Torrent J (1999a) Effect of phosphate on the crystallization of hematite, goethite and lepidocrocite from ferrihydrite. Clays Clay Miner 47(3):304–311

Gálvez N, Barrón V, Torrent J (1999b) Preparation and properties of hematite with structural phosphorus. Clays Clay Miner 47(3):375–385

Guodong Z, Takano B, Kuno A, Matsuo M (2001) Iron speciation in modern sediment from Erhai Lake, southwestern China—Redox conditions in an ancient environment. Appl Geochem 16:1201–1213

Imbernon RAL, Oliveira SMB, Blot A, Magat P (1999) Os chapéus de ferro associados ao depósito de Pb-Zn-Ag na região de Canoas, Adrianópolis (PR)—Evolução geoquímica e mineralógica. Geochim Brasil 13(2):145–161

Liang L, Korte N, Gu B, Puls R, Reeterd C (2000) Geochemical and microbial reactions affecting the long-term performance of in situ iron barriers. Adv Environ Res 4:273–286

Mitra S (1992) Applied Mössbauer spectroscopy—theory and practice for geochemists and archaeologists. Pergamon Press, Oxford, pp 381

Murad E (1998) Clays and clay minerals: what can Mössbauer spectroscopy to do help understand them? Hypn Interact 117:39–70

Murad E, Schwertmann U (1980) The Mössbauer spectrum of ferrihydrite and its relations to those of other iron oxides. Am Miner 65:1044–1049

Oliveira SMB, Imbernon RAL, Partiti CSM, Rechenberg HR (1996) Mössbauer spectroscopy study of iron oxides and oxyhydroxides in gossans. Geoderma 73:245–256

Petrovsky E, Ellwood BB (1999) Magnetic monitoring of air-, land- and water pollution. In: Maher BA, Thompson R (eds) Quaternary climates, environments and magnetism. Cambridge University Press, Cambridge, pp 279–322

Trivedi P, Axe L, Dyer J (2001) Adsorption of metal ions onto goethite: single-adsorbate and competitive systems. Colloids Surf A Physiochem Eng Aspen 191(1–2):107–121

Van der Zee C, Slomp CP, Rancourt DG, de Lange GJ, Van Raaphorst W (2005) A Mössbauer spectroscopic study of the iron redox transition in eastern Mediterranean sediments. Geochim Cosmochim Acta 69:441–453

Vandenberghe RE, De Grave E, Landuydt C, Bowen LH (1990) Some aspects concerning the characterization of iron oxides and hydroxides in soils and clays. Hypn Interact 53:175–195